

See discussions, stats, and author profiles for this publication at: <https://www.researchgate.net/publication/221963410>

Crown Ether Complexes with H_3O^+ and NH_4^+ : Proton Localization and Proton Bridge Formation

ARTICLE in THE JOURNAL OF PHYSICAL CHEMISTRY A · JUNE 2011

Impact Factor: 2.69 · DOI: 10.1021/jp200481w · Source: PubMed

CITATIONS

21

READS

73

6 AUTHORS, INCLUDING:



[Paola Hurtado](#)

Universidad Pablo de Olavide

19 PUBLICATIONS 356 CITATIONS

[SEE PROFILE](#)



[Francisco gámez](#)

Universidad Pablo de Olavide

36 PUBLICATIONS 189 CITATIONS

[SEE PROFILE](#)



[Said Hamad Gomez](#)

Universidad Pablo de Olavide

60 PUBLICATIONS 1,284 CITATIONS

[SEE PROFILE](#)



[Jeffrey D. Steill](#)

Oak Ridge National Laboratory

84 PUBLICATIONS 1,490 CITATIONS

[SEE PROFILE](#)

Crown Ether Complexes with H_3O^+ and NH_4^+ : Proton Localization and Proton Bridge Formation

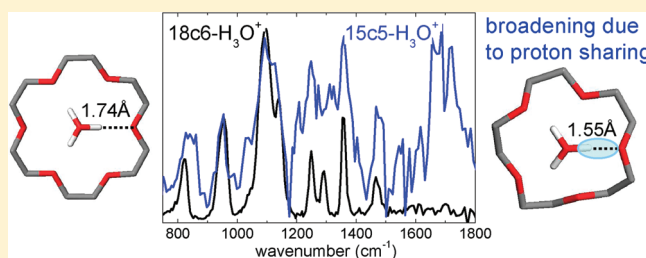
Paola Hurtado,[†] F. Gámez,[†] Said Hamad,[†] Bruno Martínez-Haya,^{*,†} Jeffrey D. Steill,[‡] and Jos Oomens^{‡,§}

[†]Departamento de Sistemas Físicos, Químicos y Naturales, Universidad Pablo de Olavide, 41013 Seville, Spain

[‡]FOM Institute for Plasma Physics Rijnhuizen, Edisonbaan 14, NL-3439 MN Nieuwegein, The Netherlands

[§]University of Amsterdam, Science Park 904, 1098XH Amsterdam, The Netherlands

ABSTRACT: The complexes formed by crown ethers with hydronium and ammonium cations are of key relevance for the understanding of their supramolecular behavior in protic solvents. In this work, the complexes of the 15-crown-5 (15c5) and 18-crown-6 (18c6) ethers with H_3O^+ and NH_4^+ and their deuterated variants are investigated under isolated conditions. The study employs infrared multiple photon dissociation (IRMPD) vibrational spectroscopy and DFT B3LYP/6-31++G(d,p) calculations for conformational assignment. The 18c6 ether provides two energetically nearby C_{3v} conformations with commensurate linear $\text{O}-\text{H}\cdots\text{O}$ and $\text{N}-\text{H}\cdots\text{O}$ bonds. The 15c5 ether ring adopts partially folded asymmetric pyramidal geometries, yielding one shorter linear H bond and two longer non-linear H bonds. Remarkably, an appreciable broadening of the IRMPD vibrational bands is observed for the $15\text{c5}-\text{H}_3\text{O}^+/\text{D}_3\text{O}^+$ complexes. This can be interpreted as a signature for partial sharing of the proton (or deuteron) between the water and the crown ether along the linear $\text{O}-\text{H}\cdots\text{O}$ intermolecular H bond, which is indeed particularly short for this complex.



I. INTRODUCTION

Crown ethers constitute a cornerstone in Macrocyclic Chemistry due to their specific binding to metal and molecular cations.^{1,2} The supramolecular complexes formed by the crown ethers with oxonium ions, $\text{H}^+(\text{H}_2\text{O})_n$,^{3–8} the ammonium ion, NH_4^+ ,^{9–16} and protonated amines, RNH_3^+ and R_2NH_2^+ ,^{17–23} constitute current active areas of fundamental and applied research. Crown ethers are known to stabilize oxonium ions of specific sizes⁸ and feature a unique capability for recognition and enantiomeric discrimination of amines and amino acids in protic solvents. In fact, a range of modern supramolecular materials, such as rotaxanes or a family of photoactive complexes, are based on these unique recognition properties of crown ethers.^{9,10,12,22}

In spite of the rapid development of the chemistry of crown ethers and its applications, basic conformational aspects of crown–hydronium and crown–ammonium complexes remain a matter of debate. The 18-crown-6 ether (18c6) features a six-oxygen cavity, matching well a C_{3v} coordination with H_3O^+ and NH_4^+ . Such coordination may involve either linear H-bonding with three oxygens of the crown ether or, alternatively, the participation of all six oxygens of the ring in “bifurcated” conformations.^{4–6,12,11} Whereas increasing experimental and theoretical evidence supports the linear binding conformation,^{4,5,7,16} the question of proton location is not trivial, and key aspects such as proton bridge formation have not been fully addressed for these systems.

Most of the previous investigations of crown ether complexes with H_3O^+ and NH_4^+ have been performed in solution or solid

phases. In those environments, the interactions with the solvent and with counterions^{4,8} pose an important challenge to the accurate description of the systems with ab initio computational methods. Complementary to condensed phase studies, modern mass spectrometry techniques allow for the routine preparation and storage of isolated ionic supramolecular complexes of well-defined stoichiometry.²⁴ A broad range of spectroscopic techniques may be then applied to characterize their conformational landscapes. A main advantage of this approach is that it can provide an in-depth insight into the intrinsic intramolecular and intermolecular interactions and the structural properties of the system, in direct connection with computational modeling. A number of gas-phase studies of crown complexes with protonated amines and amino acids have been carried out in the past decade.^{17–21} Those studies have been mainly focused on the determination of relative affinities and stoichiometries of the complexes, rather than on their structure. As an exception, coarse conformational features of polyether–amino acid complexes have been derived from ion mobility experiments,²⁰ which showed that crown ether complexes are more compact than their linear polyether analogues.

Special Issue: J. Peter Toennies Festschrift

Received: January 17, 2011

Revised: February 15, 2011

Published: March 16, 2011

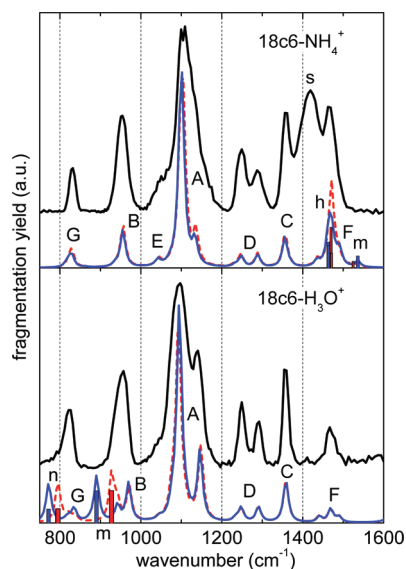


Figure 1. Infrared spectra of the 18c6-NH₄⁺ and 18c6-H₃O⁺ complexes: experimental IRMPD spectra (upper black curves in each panel) and B3LYP/6-31++G(d,p) harmonic IR spectra (lower curves; conformer I, blue solid line; conformer II, red-dash line, see Figure 4). The B3LYP spectra are convoluted with an 8 cm⁻¹ fwhm line shape function. See Table 1 for the assignment of the vibrational bands. The vertical bars indicate transitions associated with vibrational modes of the NH₄⁺ or H₃O⁺ guest.

In this study, infrared multiple photon dissociation (IRMPD) action spectroscopy is applied to characterize the isolated gas-phase complexes formed by the 18-crown-6 and 15-crown-5 ethers with H₃O⁺ and NH₄⁺. For 15-crown-5, the deuterated cationic guests are also considered. Similar previous studies have served to elucidate subtle conformational features of the alkali metal complexes of these two crown ethers.^{25–27} Methodological details are provided in section II. It will be shown that the position and broadening of the vibrational bands provide a valuable signature for the conformation of the complexes and for the questions of proton localization and proton bridge formation.^{32–39}

II. METHODOLOGY

A. Experiment. Infrared multiple photon dissociation spectra were recorded in the 750–1800 cm⁻¹ range using a FT-ICR mass spectrometer coupled to the beamline of the free electron laser FELIX.²⁸ The crown-H₃O⁺ complexes were produced via electrospray ionization of acidic solutions of the crown ether (1 mM) in a water/methanol mixture. To form the 15c5-D₃O⁺ complex, a solution in D₂O/CH₃OD with the deuterated CH₃COOD acid was employed. For the ammonium complexes, NH₃ or ND₃ were incorporated to the above solutions at 1 mM concentration. The parent ions of the complexes are pulse injected into the ICR cell, where they are mass isolated and stored at room temperature. Spectroscopic probing is carried out with laser pulses that induce fragmentative multiple photon absorption, resonant with the vibrational modes of the complex. Typically, 10 FELIX pulses are applied at each wavelength, which are approximately 5 μs long and have a pulse energy of about 40 mJ. The spectral bandwidth of the radiation amounts to about 0.5% of the central wavelength. A more detailed description of typical experimental procedures can be found in ref 29.

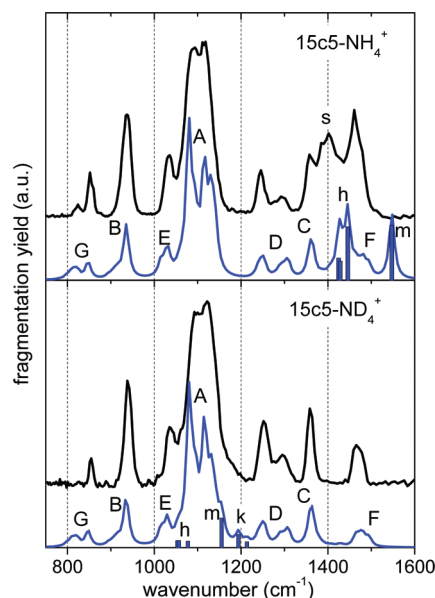


Figure 2. Infrared spectra of the 15c5-NH₄⁺ complex and its deuterated variant, 15c5-ND₄⁺: experimental IRMPD spectra (upper curves in each panel) and B3LYP/6-31++G(d,p) harmonic IR spectra of the most stable conformer I (see Figure 5). The B3LYP spectra are convoluted with an 8 cm⁻¹ fwhm line shape function. See Table 1 for the assignment of the vibrational bands. The vertical bars indicate transitions associated with vibrational modes of the NH₄⁺ or ND₄⁺ guest.

The IRMPD spectrum is constructed by monitoring the yield of the dominant fragment ion, which was in all cases the protonated crown ether formed via loss of the water or ammonia moiety of the guest cation. Less intense signals were also observed at the masses of (protonated) fragments associated with the additional loss of two or three (C₂H₄O) ether units from the crown ring. The pronounced C–O stretching band was repeatedly probed at several attenuated laser powers to avoid potential saturation due to depletion of complexes in the laser beam path. The recorded spectra were linearly corrected for the changes in laser pulse power, in consonance with the noncoherent multiple photon dissociation mechanism driving IRMPD.³⁰

B. Computations. The vibrational and conformational assignments of the spectral features observed in the experiments were performed with the aid of quantum mechanical calculations. The computational methodology is similar to the one described in ref 27. The conformational landscape of the complexes was explored by means of simulated annealing with the Dreiding force field. After discriminating duplicate molecular structures, the ~10 lowest energy conformers of each complex were selected for further optimization. In addition, the (nonduplicate) structures resulting from the exchange of NH₄⁺ and H₃O⁺ in each complex were also considered. The resulting structures were optimized with density functional theory (DFT) at the B3LYP/6-31++G-(d,p) level. The counterpoise method was applied to reduce the basis set superposition error. No symmetry constraints were imposed to the conformers. All the calculations were carried out with the Gaussian 03 code.⁴¹ The free energies reported in this work account for the electronic energy plus thermal and vibrational zero-point energy corrections. Theoretical harmonic IR spectra were generated by convoluting the normal modes of vibration of the optimized structures with a line broadening function of 8 cm⁻¹ fwhm. The computed vibrational frequencies

for all the complexes were scaled for comparison with experiment by a factor 0.98, in line with the scaling recommended for the B3LYP/6-31++G(d,p) method from previous studies.³¹

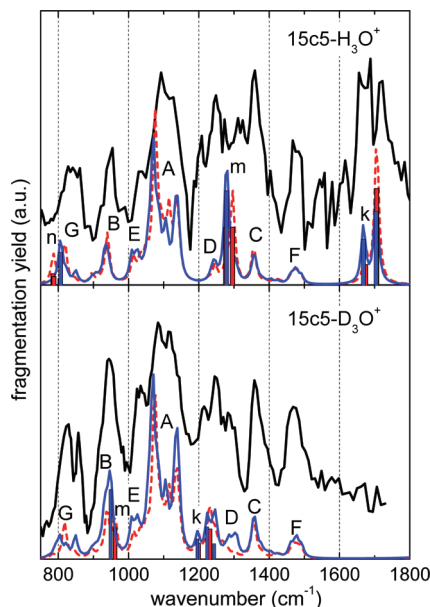


Figure 3. Infrared spectra of the 15c5–H₃O⁺ complex and its deuterated variant, 15c5–D₃O⁺: experimental IRMPD spectra (upper black curves in each panel) and B3LYP/6-31++G(d,p) harmonic IR spectra of the two most stable conformers (lower curves; conformer I, blue solid line; conformer II, red-dash line, see Figure 5). The B3LYP spectra are convoluted with an 8 cm^{−1} fwhm line shape function. See Table 1 for the assignment of the vibrational bands. The vertical bars indicate transitions associated to vibrational modes of the H₃O⁺ or D₃O⁺ guest. The enhanced broadening of the IRMPD spectra for the 15c5–hydronium system may be interpreted as a signature for partial proton delocalization along the shortest host–guest H-bond.

III. RESULTS AND DISCUSSION

Figures 1, 2, and 3 show the IRMPD spectra of the complexes investigated in this work. The corresponding B3LYP/6-31++G(d,p) harmonic IR spectra of the one or two lowest energy conformers likely to have a relevant contribution are also shown for direct comparison. The molecular structures of such conformers are depicted in Figures 4 and 5. As described below in detail, all the conformers involve a tripodal coordination of the cationic guest with three oxygens of the crown ether ring. Evidence for bifurcated coordination, in which one O–H or N–H bond of the guest cation interacts with a pair of crown oxygens in a roughly symmetric way, was only found for some of the higher energy conformers of the 15-crown-5 complexes (for example, 15c5–NH₄⁺ conformer II in Figure 5). Also, importantly, no molecular arrangements with a coordination number different than three were found in our study within 40 kJ mol^{−1} above the most stable conformer. For instance, a specific test showed that folded cage-like conformers with a 4-fold coordination of the 18c6 and 15c5 crown rings with the NH₄⁺ guest were unstable and systematically migrated to more open tripodal arrangements upon B3LYP/6-31++G(d,p) geometry optimization.

Each of the IRMPD spectra displays a series of differentiated vibrational bands. The most prominent bands can be assigned to vibrational modes of the crown ether host (bands labeled with capital letters, A–G), as described in Table 1. The crown backbone vibrations involve C–O–C (A) and C–C (B) stretching along the ring, as well as wagging (C), twisting (D), bending (E), and rocking (F) motions of the CH₂ groups.^{25–27} The position and shape of these bands constitute probes for the conformational features of the crown ether host and its coordination with the protonated guest. In particular, the shape of the intense C–O–C stretching band A changes appreciably from one type of complex to the other. This is mainly due to the different splitting of the three to four main components that

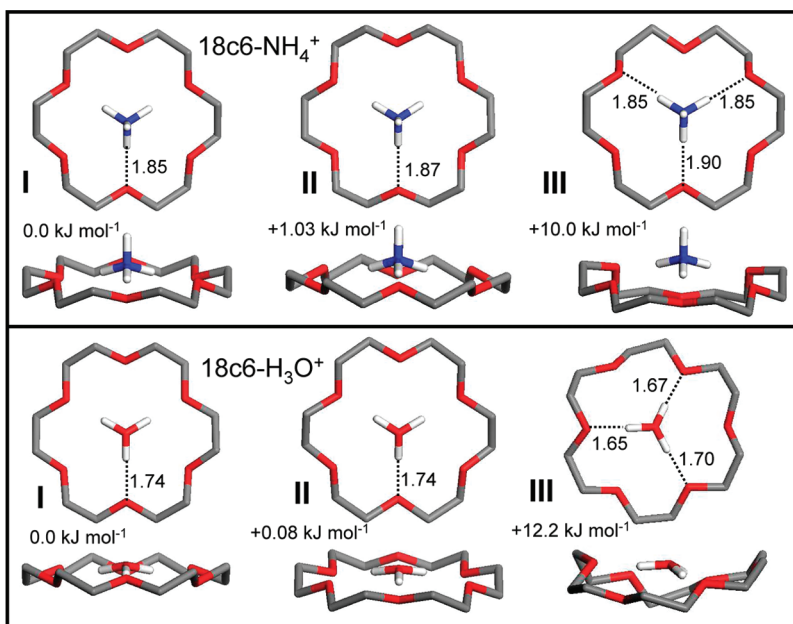


Figure 4. Graphical representation of the B3LYP/6-31++G(d,p) equilibrium geometry of the most stable conformers of the 18c6 complexes with NH₄⁺ and H₃O⁺: oxygens in red, carbons in gray, guest hydrogens in white. The crown ether hydrogens have been omitted for clarity. The shortest (guest)H⁺⋯O(crown) distances (in Å) are indicated in the graphs; an extended list of geometrical parameters is provided in Table 2.

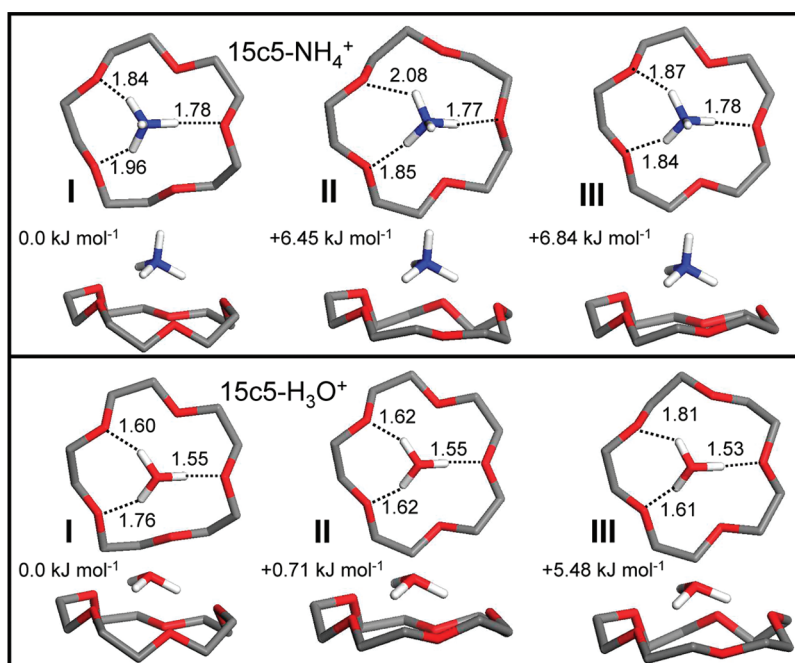


Figure 5. Graphical representation of the B3LYP/6-31++G(d,p) equilibrium geometry of the most stable conformers of the 15c5 complexes with NH_4^+ and H_3O^+ : oxygens in red, carbons in gray, guest hydrogens in white. The crown ether hydrogens have been omitted for clarity. The shortest (guest) $\text{H}^+ \cdots \text{O}(\text{crown})$ distances (in Å) are indicated in the graphs; an extended list of geometrical parameters is provided in Table 2.

make up the band in the different coordination arrangements, which is well accounted for by the B3LYP calculations.

A set of vibrational modes dominantly associated with the protonated guests also enter the spectral range covered by the present measurements (bands labeled with lower-case letters, h–s). According to the B3LYP calculation (see Table 1), such modes can be described as umbrella motions of H_3O^+ or NH_4^+ (h,m), as bending of H_2O or NH_2 bond angles (k), and as twisting of an H_2O group around the axis of the third O–H bond (n). The positions of these bands are shown as vertical bars in Figures 1–3, which helps in their identification and in the appreciation of the consistent shift to lower frequencies associated with the deuteration of the guest cation. Inspection of the B3LYP harmonic motions reveals that the guest modes couple easily with the CH_2 ether groups. In particular, the vibrational mode h (the umbrella motion parallel to the crown ring) in the $15\text{c}5\text{--NH}_4^+$ complex splits into two main components (Figure 2) that can be attributed to coupling with either the bending or wagging CH_2 modes.

Noticeably, some of the vibrational modes of the protonated guests predicted by the B3LYP harmonic computation appear to be absent in the recorded IRMPD spectra. This effect is apparent at least for the mode labeled m (umbrella perpendicular to the ring), and can be interpreted as a signature for anharmonic effects associated with large amplitude motions of the H_3O^+ and NH_4^+ moieties within the restricted environment provided by the host–guest coordination network. Anharmonic vibrational modes are likely to induce band shifts and broadenings that are known to be ill–characterized by harmonic frequency calculations, see, for example, the case of aniline.⁴³ Moreover, their multiple photon excitation may be less efficient in IRMPD experiments.³⁹

Conversely, a broad band not predicted by the B3LYP calculations is observed in the IRMPD spectra of the 18c6 and

Table 1. Vibrational Mode Assignment from the B3LYP/6-31++G(d,p) Calculation for the Main Bands Observed in the IRMPD Spectra of This Work^a

band	mode assignment
Vibrational Modes of Crown Host	
A	C–O stretching ; C–C stretching, CH_2 rocking, OCCO torsions,
B	C–C stretching ; CH_2 rocking, COC bending
C	CH_2 wagging
D	CH_2 twisting
E	C–C stretching ; C–O stretching
F	CH_2 bending
G	CH_2 rocking ; COC bending
Vibrational Modes of Guest Cation	
h	NH_4^+ umbrella (parallel to crown ring)
k	NH_2 or OH_2 bending
m	NH_4^+ or H_3O^+ umbrella (normal to crown ring)
n	OH_2 twisting
s	NH_4^+ stretching (tentative from ref 36 and 37)

^aThe dominant type of vibration (in boldface) and significant secondary types of vibration are indicated in each case. Bands are labelled with capital letters, “A” through “G”, for the modes dominated by vibrations of the crown host, and with low case letters, “h” through “s”, for modes predominantly associated with vibrations of the protonated guest.

15c5 complexes with NH_4^+ at around 1400 cm^{-1} (band s). This band clearly vanishes in the $15\text{c}5\text{--ND}_4^+$ complex, which corroborates that it is associated with the ammonium guest. Based on multidimensional quantum calculations, bands observed in this same spectral range in the IRMPD spectra of protonated ammonia clusters have been assigned to symmetric and antisymmetric stretching modes.^{36,37} Similar calculations for the present

Table 2. Selected Geometrical Parameters for the Three Lowest Energy B3LYP/6-31++G(d,p) Conformers of the 15c5 and 18c6 Complexes with NH_4^+ and H_3O^+ (Conformers I, II, and III in Figures 4 and 5)^a

conformer	$\text{NH}^+ \cdots \text{O}(\text{crown})$ or $\text{OH}^+ \cdots \text{O}(\text{crown})$ distances (Å)	crown O—O distances (Å)	C—O—C bond angles	O—C—C—O dihedral angles
18c6- NH_4^+ I (C_{3v}) 0 kJ mol ⁻¹	(1.85, 2.56)	2.86	112.9, 114.0	65.5, -65.5
18c6- NH_4^+ II (C_{3v}) 1.03 kJ mol ⁻¹	(1.87, 2.55)	2.87	113.6, 113.2	-66.0, 66.0
18c6- NH_4^+ III (C_s) 10.5 kJ mol ⁻¹	(1.85, 2.60),	2.89, 2.85,	115.3, 113.5,	-62.1, 65.0,
	(1.85, 2.57),	2.85, 2.89,	113.4, 113.5,	-64.7, 62.6,
	(1.90, 2.59)	2.85, 2.85	115.3, 113.3	65.4, -66.1
18c6- H_3O^+ I (C_{3v}) 0 kJ mol ⁻¹	(1.74, 2.54)	2.81	112.1, 113.8	63.6, -63.7
18c6- H_3O^+ II (C_{3v}) 0.08 kJ mol ⁻¹	(1.74, 2.54)	2.81	112.1, 113.9	-63.5, 63.5
18c6- H_3O^+ III (C_1) 12.2 kJ mol ⁻¹	(1.65, 2.55)	2.87, 2.73	114.9, 115.2	-65.8, 55.7
	(1.67, 2.52)	2.76, 2.84	112.9, 114.5	57.9, -66.6
	(1.70, 2.54)	2.80, 2.80	112.5, 113.8	61.9, 63.6
15c5- NH_4^+ I (C_1) 0 kJ mol ⁻¹	(1.78, 2.58)	2.91, 2.85	115.0, 113.9	-63.3, 58.6
	(1.96, 2.36)	3.00, 2.82	115.2, 115.1	70.1, 64.9,
	(1.84, 2.54)	2.81	115.2	-63.6
15c5- NH_4^+ II (C_1) 6.45 kJ mol ⁻¹	(1.77, 2.60)	2.83, 2.77	114.9, 115.7	65.9, -60.2
	(1.85, 2.53)	2.92, 2.83	113.6, 116.6	59.0, 60.6
	(2.08, 2.24)	2.96	115.6	69.0
15c5- NH_4^+ III (C_1) 6.84 kJ mol ⁻¹	(1.78, 2.54)	2.80, 2.80	114.3, 116.3	61.4, -63.7
	(1.84, 2.41)	2.99, 2.82	113.9, 116.1	65.3, 65.6
	(1.87, 2.47)	2.81	115.6	-60.8
15c5- H_3O^+ I (C_1) 0 kJ mol ⁻¹	(1.55, 2.52)	2.88, 2.78	115.2, 115.3	-63.6, 56.1
	(1.76, 2.27)	3.00, 2.78	115.8, 115.8	70.4, 63.5
	(1.60, 2.42)	2.80	115.9	63.4
15c5- H_3O^+ II (C_1) 0.71 kJ mol ⁻¹	(1.55, 2.49)	2.81, 2.77	114.2, 116.6	62.2, -63.1
	(1.62, 2.31)	3.00, 2.78	114.9, 116.7	67.2, 64.4
	(1.62, 2.38)	2.80	116.1	-61.0
15c5- H_3O^+ III (C_1) 5.48 kJ mol ⁻¹	(1.53, 2.54)	2.82, 2.75	115.5, 116.1	65.5, -60.1
	(1.61, 2.39)	2.95, 2.76	114.1, 117.1	61.2, 56.4
	(1.81, 2.21)	2.92	116.6	67.4

^a The series starts with the crown oxygen atom closest to a proton and proceeds clockwise according to the top view representations of the conformers in Figures 4 and 5. The entries in parentheses in the second column correspond to the distances between the H atoms of the protonated guest and the two closest oxygen atoms of the crown ring. The last three columns refer to the crown ether backbone exclusively. Conformers have symmetries belonging to the C_{3v} , C_s , and C_1 point groups, as indicated in the first column. For the C_{3v} conformers, the tabulated values are 3-fold or 6-fold repeated.

complexes are well beyond the scope of this study and it is thus not straightforward to assign the observed bands in a similar fashion. Alternatively, bands s may correspond to anharmonically shifted bands (for example, m and h in the computed spectrum).

The IRMPD spectra for 18c6- NH_4^+ , 18c6- H_3O^+ , and 15c5- NH_4^+ /ND₄⁺ systems show well-defined vibrational structures that are accurately reproduced by the calculated harmonic IR spectrum. In marked contrast, the IRMPD spectra observed for 15c5- H_3O^+ and 15c5-D₃O⁺ display complex broadened band structures. In spite of the noisy appearance of these latter spectra, the observed band features were consistently reproduced in independent scans performed with different sample solutions and chemicals, and at different laser powers. The differences between the 15c5- H_3O^+ /D₃O⁺ spectra and those of the rest of the systems presently investigated are indeed remarkable. The main spectral bands are still recognizable but are spread over a broader spectral range and show substantial changes in their structure and relative intensities. This finding constitutes an evidence for vibrational couplings leading to new channels for internal energy redistribution during the IRMPD process. In fact, qualitatively similar band shifts and non-homogeneous

broadenings, not matching the harmonic calculations, have been observed in previous IRMPD investigations of proton bound complexes,^{32,35–37,39,40,44,45} in particular, involving ethers.^{32,45} Based on those previous studies, the spectral features observed here for 15c5- H_3O^+ /D₃O⁺ can be plausibly attributed to partial proton delocalization along the O \cdots H \cdots O intermolecular bonds of the complex. This key aspect is discussed below in more detail.

The inspection of the most stable B3LYP conformers provides a deeper insight into the location of the charge and the potential proton bridge formation in the host–guest hydrogen bonds formed in each of the complexes investigated. Figures 4 and 5 and Table 2 describe the B3LYP molecular structures of these conformers, which are supported by the good agreement between the experimental IRMPD spectra and the calculated bands associated with the crown backbone vibrations. The 18c6- H_3O^+ /NH₄⁺ complexes are stabilized in conformations of C_{3v} symmetry, featuring three roughly linear hydrogen bonds. The alternative conformations in which the H bonds are bifurcated between two adjacent ether oxygens were found to correspond to saddle points rather than to local minima in our

calculations. These results are in agreement with previous studies.^{3–5}

The 18c6–H₃O⁺ complex displays two roughly isoenergetic C_{3v} conformers (I and II in Figure 4) in which the hydronium lies only slightly above the plane of the open crown backbone and coordinates either with the three ether oxygens pointing upward (toward the cation) or with the three oxygens pointing downward. Interestingly, interconversion between these conformers may be achieved either by rotation or by inversion of the H₃O⁺ moiety. The 18c6–NH₄⁺ complex displays two conformers with similar features but with a more pyramidal shape and larger interatomic distances in the hydrogen bonds. The two conformers are in this case slightly further apart in relative energy, though only by 1 kJ/mol. The most stable conformer corresponds to a slightly deeper inclusion of the ammonium into the crown cavity, forming a tripodal H-bonding coordination with the ether oxygens pointing downward with respect to the position of the guest. The small difference in free energy between the conformers of each of the 18c6 complexes suggests that the experimental IRMPD spectra, collected at room temperature, should be compared to the average of the two B3LYP spectra shown in Figure 1. The conformers next in energy for both 18c6–H₃O⁺ and 18c6–NH₄⁺, adopt partially folded conformations (conformers III in Figure 4) and lie more than 10 kJ mol^{–1} above the C_{3v} conformers. Incidentally, conformer III for 18c6–H₃O⁺ is almost isoenergetic with a fourth conformer of C_s symmetry (not shown), which is qualitatively similar to the C_s conformer III for 18c6–NH₄⁺.

The 15c5–H₃O⁺/NH₄⁺ complexes are stabilized in nonplanar asymmetric conformations driven by the nonmatching symmetries of the host and the guest. Due to the additional complexity caused by such geometrical incommensurability, a particularly extensive conformational search was performed for these systems. Figure 5 shows that the most stable conformers I, II, and III for NH₄⁺ and H₃O⁺ are qualitatively similar, although with differences in their relative free energies. It is worth mentioning that their conformational features are in qualitative accordance with those postulated for the 15c5–H₃O⁺ complex in dichloroethane solution.³ All conformers feature one roughly linear hydrogen bond (ca. 175°) and two bent hydrogen bonds (140–165° for H₃O⁺; 125–165° for NH₄⁺) between the crown oxygens and the cation. Only three of the ether oxygens are involved in the binding of the cation, leaving two oxygen sites at longer distances from the guest H-ends. Only for conformer II of 15c5–NH₄⁺ one of the H bonds is partially shared by two oxygens differing by 0.16 Å in their distances to the N–H bond.

The linear H bond in the 15c5 complexes is also systematically the shortest one. Due to this bond asymmetry, the charge density on the proton involved in the linear bond is larger than that on the other guest H-atoms. Conformers I, II, and III of the 15c5–H₃O⁺ complex feature a particularly short linear hydrogen bond of about 1.55 Å, with a distance between the water oxygen and the ether oxygen of 2.56 Å. The analogous interatomic distances for the 15c5–NH₄⁺ complex amount to about 1.78 and 2.81 Å, and for the 18c6–H₃O⁺ complex to 1.74 and 2.73 Å. Hence, only the 15c5–H₃O⁺ system presents interatomic distances typical of a strong O–H⁺⋯O hydrogen bond.⁴² Such distances are in fact similar to those found for, for example, the HOH⋯OH^{–33} and HOH⋯O^{–34} systems. In contrast, the longer H–bond distances in the 15c5–NH₄⁺ and the 18c6–H₃O⁺/NH₄⁺ complexes are closer to those of prototypical H bonds of intermediate strength.⁴² These findings,

together with the smaller proton affinity of water in comparison to ammonia, supports the occurrence of host–guest proton sharing in the 15c5–H₃O⁺ system.

According to the present observations, proton delocalization effects are strong enough as to appreciably broaden the IRMPD bands in the 15c5–H₃O⁺ system. The delocalization of the proton in the bond affects the bulk of the vibrational modes of the complex, due to their coupling with the large amplitude anharmonic vibrational motion of the (partially) shared proton. The impact of proton delocalization on IRMPD spectroscopy has been described in detail by means of quantum ab initio molecular dynamics for related systems, in particular, for proton-bridged ether dimers.^{40,44,45} Those theoretical studies have explained the shifts, splittings and overall broadenings of the IRMPD vibrational bands in terms of the dynamic coupling between the shared proton and the “bath” of vibrational modes of the complex. Such coupling drives a temperature-dependent modulation that smoothly transforms the narrow bands observed in single-photon spectra at low temperature into the complex broadened structure of the IRMPD spectra recorded at room temperature.⁴⁵ The fact that IRMPD broadening effects are observed in the present study only for 15c5–H₃O⁺/D₃O⁺ is consistent with the tight H–bonding predicted by the B3LYP computation. It seems difficult to invoke alternative mechanisms, not involving proton sharing, that would differentiate so sharply the IRMPD behavior of 15c5–H₃O⁺ in comparison to 15c5–NH₄⁺, 18c6–H₃O⁺, and 18c6–NH₄⁺. In particular, our conformational survey did not find any evidence for the participation of multiple conformers, that could potentially account for a spread of the vibrational bands in the present IRMPD measurements. As shown in Figure 5, the two conformers predicted to have a relevant contribution at room temperature do not explain the observed band widths.

IV. SUMMARY AND CONCLUSIONS

The combination of IRMPD spectroscopy and B3LYP computations has served to obtain novel insights into the complexes formed by the 18c6 and 15c5 crown ethers with H₃O⁺ and NH₄⁺ under isolated conditions. The results confirm an open C_{3v} commensurate coordination of the 18c6 crown ether with both H₃O⁺ and NH₄⁺, involving three linear H-bonds. In the 15c5 complexes, the ether ring adopts partially folded conformations leading to asymmetric pyramidal geometries in its coordination with the cation. As a main feature, the 15c5 complexes display one shorter linear H bond and two longer non-linear H bonds.

The (guest)O/N–H⁺⋯O(ether) coordination features interatomic distances typical of hydrogen bonds of intermediate strength. Proton sharing appears to be negligible in the 15c5–NH₄⁺, 18c6–H₃O⁺ and 18c6–NH₄⁺ complexes, all of which display well-defined IRMPD bands in good accord with the B3LYP prediction. In contrast, the 15c5–H₃O⁺ complex features a tighter binding and a stronger H bonding is predicted at least along the shortest linear bond. Substantial changes in the intensities, broadening and general shape of the IRMPD vibrational bands differentiates the 15c5–H₃O⁺ and 15c5–D₃O⁺ complexes. These spectral features can be interpreted as a signature for partial proton delocalization along the linear H bond. Such interpretation is supported by the similar spectral effects observed in previous studies on systems with shared protons.^{32,35–37,39,40,44,45} The wave function of the shared proton can be expected to concentrate on the shortest linear H-bond of

the $15\text{cS}-\text{H}_3\text{O}^+$ complex. Nevertheless, proton delocalization may have a dynamic character modulated by the internal stretching motions of the hydronium guest, and also involve the longer nonlinear bonds. The accurate description of these features would require multidimensional quantum calculations.^{44,45} Further advances would also benefit from additional spectroscopic experiments probing the C–H/O–H/N–H stretching regions, for example, employing the single photon techniques that have served to characterize the conformational landscapes of isolated and solvated crown–metal complexes.^{46–49}

As a general consideration, the present study corroborates that the sensitivity of IRMPD spectroscopy to anharmonicity and vibrational coupling effects serves as a qualitative probe for proton delocalization effects, in particular, in proton-mediated supramolecular complexes of ethers and related compounds.

AUTHOR INFORMATION

Corresponding Author

*E-mail: bmarhay@upo.es.

ACKNOWLEDGMENT

B.M.H. is indebted to J.P. Toennies and M. Faubel for their guidance during the early stages of his scientific career at Max–Planck Institut für Strömungsforschung (Göttingen, Germany). The research leading to these results is supported by the European Community Seventh Framework Programme (FP7/2007–2013, Grant 226716). Funding was also provided by research programmes of Andalusia (P07-FQM-02600, P09-FQM-4938) and Spain (CTQ2009-10477, CSD2009-00038). J.O. acknowledges support by the Stichting Physica. The skillful assistance of Dr. B. Redlich and Dr. AFG van der Meer as well as others of the FELIX staff is gratefully acknowledged.

REFERENCES

- Pedersen, C. J. *Science* **1988**, *241*, 536.
- Gokel, G. W. *Crown Ethers and Cryptands*; Royal Society of Chemistry: London, 1994; ISBN: 978-0851867045.
- Varnek, A.; Wipff, G.; Famulari, A.; Raimondi, M.; Vorob'eva, T.; Stoyanov, E. J. *Chem. Soc., Perkin Trans.* **2002**, *2*, 887.
- Bühl, M.; Wipff, G. J. *Am. Chem. Soc.* **2002**, *124*, 4473.
- Bühl, M.; Ludwig, R.; Schurhammer, R.; Wipff, G. J. *Phys. Chem. A* **2004**, *108*, 11463.
- Stoyanov, E. S.; Reed, C. A. J. *Phys. Chem. A* **2004**, *108*, 907.
- Kriz, J.; Dybal, J.; Makrlík, E.; Budka, J. J. *Phys. Chem. A* **2008**, *112*, 10236.
- Junk, P. C. *New J. Chem.* **2008**, *32*, 762.
- Cantrill, S. J.; Fulton, D. A.; Heiss, A. M.; Pease, A. R.; Stoddart, J. F.; White, A. J. P.; Williams, D. J. *Chem.—Eur. J.* **2000**, *6*, 2274.
- Jones, J. W.; Gibson, H. W. J. *Am. Chem. Soc.* **2003**, *125*, 7001.
- Bokare, A. D.; Patnaik, A. J. *Phys. Chem. A* **2005**, *109*, 1269.
- Nierengarten, J. F.; Hahn, U.; Figueira-Duarte, T. M.; Cardinali, F.; Solladié, N.; Walther, M. E.; Van Dorselaer, A.; Herschbach, H.; Leize, E.; Albrecht-Gary, A. M.; Trabolsi, A.; Elhabiri, M. C. R. *Chim.* **2006**, *9*, 1022.
- Endicott, Ch.; Strauss, H. L. J. *Phys. Chem. A* **2007**, *111*, 1236.
- Buschmann, H. J.; Mutihac, R. C.; Schollmeyer, E. *Thermochim. Acta* **2008**, *472*, 17.
- Ehala, S.; Toman, P.; Makrlík, E.; Kasicka, V. J. *Chromatogr., A* **2009**, *1216*, 7927.
- Toman, P.; Makrlík, E.; Vanura, P. *Monatsh. Chem.* **2010**, *141*, 301.
- Williamson, B. L.; Creaser, C. S. *Int. J. Mass Spectrom.* **1999**, *188*, 53.
- Julian, R. R.; Beauchamp, J. L. *Int. J. Mass Spectrom.* **2001**, *210/211*, 613.
- Schäfer, M. *Angew. Chem., Int. Ed.* **2003**, *42*, 1896.
- Colgrave, M. L.; Bramwell, C. J.; Creaser, C. S. *Int. J. Mass Spectrom.* **2003**, *229*, 209.
- Franski, R.; Schroeder, G.; Kamysz, W.; Niedzialkowski, P.; Ossowski, T. J. *Mass Spectrom.* **2007**, *42*, 459.
- Schneider, H. J. *Angew. Chem., Int. Ed.* **2009**, *48*, 3924.
- Nagata, H.; Nishi, H.; Kamiguchi, M.; Ishida, T. *Chirality* **2008**, *20*, 820.
- Schermann, J. P. *Spectroscopy and Modelling of Biomolecular Building Blocks*; Elsevier: Amsterdam, 2008; ISBN: 978-0-444-52708-0.
- Martínez-Haya, B.; Hurtado, P.; Hortal, A. R.; Steill, J. D.; Oomens, J.; Merkl, P. J. J. *Phys. Chem. A* **2009**, *113*, 7748.
- Martínez-Haya, B.; Hurtado, P.; Hortal, A. R.; Hamad, S.; Steill, J. D.; Oomens, J. J. *Phys. Chem. A* **2010**, *114*, 7048.
- Hurtado, P.; Hortal, A. R.; Gámez, F.; Hamad, S.; Martínez-Haya, B. *Phys. Chem. Chem. Phys.* **2010**, *12*, 13752.
- <http://www.rijnh.nl/felix/>.
- Polfer, N. C.; Oomens, J. *Phys. Chem. Chem. Phys.* **2007**, *9*, 3804.
- Polfer, N. C.; Oomens, J. *Mass Spectrom. Rev.* **2009**, *28*, 468.
- Fairchild, S. Z.; Bradshaw, C. F.; Su, W.; Guharay, S. K. *Appl. Spectrosc.* **2009**, *63*, 733.
- Moore, D. T.; Oomens, J.; van der Meer, L.; von Helden, G.; Meijer, G.; Valle, J.; Marshall, A. G.; Eyler, J. R. *ChemPhysChem* **2004**, *5*, 740.
- Diken, E. G.; Headrick, J. M.; Roscioli, J. R.; Bopp, J. C.; Johnson, M. A.; McCoy, A. B. J. *Phys. Chem. A* **2005**, *109*, 1487.
- Roscioli, J. R.; Diken, E. G.; Johnson, M. A.; Horvath, S.; McCoy, A. B. J. *Phys. Chem. A* **2006**, *110*, 4943.
- Roscioli, J. R.; McCunn, L. R.; Johnson, M. A. *Science* **2007**, *316*, 249.
- Asmis, K. R.; Yang, Y.; Santambrogio, G.; Brümmer, M.; McCunn, L. R.; Roscioli, J. R.; Johnson, M. A.; Kühn, O.; Goebbert, D. J. *Angew. Chem., Int. Ed.* **2007**, *46*, 8691.
- Yang, Y.; Kühn, O.; Santambrogio, G.; Goebbert, D. J.; Asmis, K. R. J. *Chem. Phys.* **2008**, *129*, 224302.
- McCunn, L. R.; Roscioli, J. R.; Johnson, M. A.; McCoy, A. B. J. *Phys. Chem. B* **2008**, *112*, 321.
- Oomens, J.; Steill, J. D.; Redlich, B. J. *Am. Chem. Soc.* **2009**, *131*, 4310.
- Li, X.; Moore, D. T.; Iyengar, S. S. J. *Chem. Phys.* **2008**, *128*, 184308.
- Frisch, M. J.; Trucks, G. W.; Schlegel, H. B.; Scuseria, G. E.; Robb, M. A.; Cheeseman, J. R.; Montgomery, J. A.; Vreven, T.; Kudin, K. N.; Burant, J. C.; Millam, J. M.; Iyengar, S. S.; Tomasi, J.; Barone, V.; Mennucci, B.; Cossi, M.; Scalmani, G.; Rega, N.; Petersson, G. A.; Nakatsuji, H.; Hada, M.; Ehara, M.; Toyota, K.; Fukuda, R.; Hasegawa, J.; Ishida, M.; Nakajima, T.; Honda, Y.; Kitao, O.; Nakai, H.; Klene, M.; Li, X.; Knox, J. E.; Hratchian, H. P.; Cross, J. B.; Bakken, V.; Adamo, C.; Jaramillo, J.; Gomperts, R.; Stratmann, R. E.; Yazyev, O.; Austin, A. J.; Cammi, R.; Pomelli, C.; Ochterski, J. W.; Ayala, P. Y.; Morokuma, K.; Voth, G. A.; Salvador, P.; Dannenberg, J. J.; Zakrzewski, V. G.; Dapprich, S.; Daniels, A. D.; Strain, M. C.; Farkas, O.; Malick, D. K.; Rabuck, A. D.; Raghavachari, K.; Foresman, J. B.; Ortiz, J. V.; Cui, Q.; Baboul, A. G.; Clifford, S.; Cioslowski, J.; Stefanov, B. B.; Liu, G.; Liashenko, A.; Piskorz, P.; Komaromi, I.; Martin, R. L.; Fox, D. J.; Keith, T.; Al-Laham, M. A.; Peng, C. Y.; Nanayakkara, A.; Challacombe, M.; Gill, P. M. W.; Johnson, B.; Chen, W.; Wong, M. W.; Gonzalez, C.; Pople, J. A. *Gaussian 03*, Revision C.02; Gaussian, Inc.: Wallingford, CT, 2004.
- Gilli, P.; Bertolasi, V.; Ferretti, V.; Gilli, G. J. *Am. Chem. Soc.* **1994**, *116*, 909.
- Sinclair, W. E.; Pratt, D. W. J. *Chem. Phys.* **1996**, *105*, 7942.
- Iyengar, S. S. *Int. J. Quantum Chem.* **2009**, *109*, 3798.

- (45) Li, X.; Oomens, J.; Eyler, J. R.; Moore, D. T.; Iyengar, S. S. *J. Chem. Phys.* **2010**, *132*, 244301.
- (46) Rodriguez, J. D.; Lisy, J. M. *Int. J. Mass Spectrom.* **2009**, *283*, 135.
- (47) Rodriguez, J. D.; T.D. Vaden, T. D.; Lisy, J. M. *J. Am. Chem. Soc.* **2009**, *131*, 17277.
- (48) Rodriguez, J. D.; Lisy, J. M. *J. Phys. Chem. A* **2009**, *113*, 6462.
- (49) Rodriguez, J. D.; Kim, D.; Tarakeshbar, P.; Lisy, J. M. *J. Phys. Chem. A* **2010**, *114*, 1514.